Journal of ELECTRONIC MATERIALS
DOI: 10.1007/s11664-011-1885-5

Printed Se-Doped MA *n*-Type Bi_2Te_3 Thick-Film Thermoelectric Generators

DEEPA MADAN,[1,3] ALIC CHEN,[1] PAUL K. WRIGHT,[1] and JAMES W. EVANS[2]

1.—Department of Mechanical Engineering, University of California, Berkeley, CA, USA. 2.—Department of Materials Science and Engineering, University of California, Berkeley, CA, USA. 3.—e-mail: deepam@berkeley.edu

In this work, we highlight new materials processing developments and fabrication techniques for dispenser-printed thick-film single-element thermoelectric generators (TEG). Printed deposition techniques allow for low-cost and scalable manufacturing of microscale energy devices. This work focuses on synthesis of unique composite thermoelectric systems optimized for low-temperature applications. We also demonstrate device fabrication techniques for high-density arrays of high-aspect-ratio planar single-element TEGs. Mechanical alloyed (MA) *n*-type Bi_2Te_3 powders were prepared by taking pure elemental Bi and Te in 36:64 molar ratio and using Se as an additive. X-ray diffraction (XRD) and scanning electron microscopy (SEM) techniques were used to characterize the as-milled powders to confirm the Bi_2Te_3 phase formation and particle size below 50 μm. Thermoelectric properties of the composites were measured from room temperature to 100°C. We achieved a dimensionless figure of merit (ZT) of 0.17 at 300 K for MA *n*-type Bi_2Te_3–epoxy composites with 2 wt.% Se additive. A 20 single-leg TEG prototype with 5 mm × 400 μm × 120 μm printed element dimensions was fabricated on a polyimide substrate with evaporated gold contacts. The prototype device produced a power output of 1.6 μW at 40 μA and 40 mV voltage for a temperature difference of 20°C.

Key words: Thermoelectric, energy harvesting, mechanical alloy dispenser printing, polymer composites

INTRODUCTION

Thermoelectric generators (TEGs), devices that convert thermal energy directly into electrical energy, are potential power sources for autonomous microsystems. A TEG utilizes heat flow to form a temperature gradient across solid-state materials, providing power to an electrical load. The temperature difference across a TEG provides a voltage potential ($V = \alpha\Delta T$) from the Seebeck effect (Seebeck coefficient, α).[1] Efficient TEGs require fabrication of high-density, high-aspect-ratio semiconductor elements placed electrically in series and thermally in parallel.[2] TEGs manufactured using standard microfabrication techniques are frequently limited to low-aspect-ratio elements due to limitations of evaporation and sputtering techniques. By utilizing a planar device design, efficient TEGs can be fabricated on electrically insulating substrates.[3,4] Planar high-density array devices can be rolled into a compact form factor if devices are printed on flexible substrates.[4] Films deposited on flexible substrates, however, require long fatigue life to prevent cracking.[5]

Dispenser printing techniques meet the requirements for fabrication of planar TEG devices on flexible substrates. Figure 1 shows a schematic of a single-element TEG device manufactured using a dispenser printer. While traditional TEGs utilize a set of complementary *n*-type and *p*-type thermoelectric materials, a single-element device (consisting of

(Received July 17, 2011; accepted December 21, 2011)

Published online: 25 January 2012

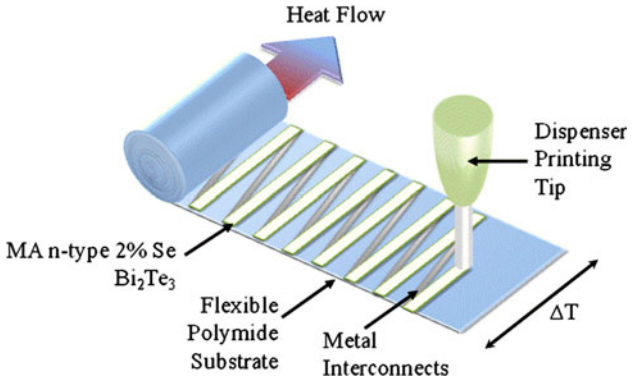

Fig. 1. Schematic of a planar single-element thermoelectric device with printed active thermoelectric material.

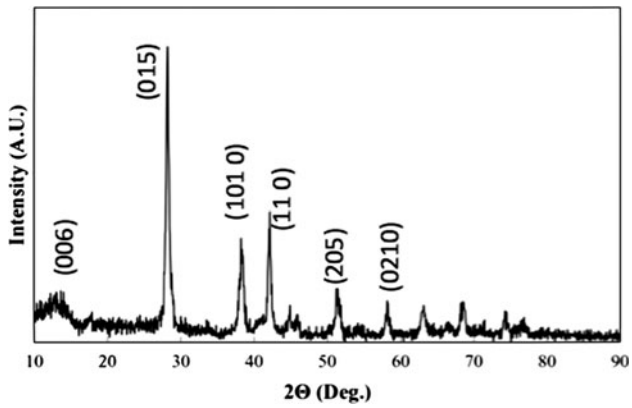

Fig. 2. XRD pattern of MA *n*-type Bi_2Te_3 with 2% Se sample.

either *n*-type or *p*-type) can also be fabricated by utilizing metal electrical interconnects spanning from the top of one element to the base of the next element. In effect, the metal interconnect acts as the complementary material in the thermocouple. Printing typically involves use of synthesized thermoelectric inks that consist of active materials in polymer binders and solvents.[4,6] Printing eliminates the need for expensive processing steps such as lithography, physical and chemical vapor deposition, and etching that are commonly employed in standard microfabrication techniques. It utilizes additive processing steps, thus reducing material waste and cost per unit area compared with standard technologies.

We utilize a custom-developed dispenser printer to print high-aspect-ratio planar single-element TEGs. The printer has been successfully used in battery, capacitor, and microelectromechanical systems (MEMS) research.[7–9] Although the printer is used for prototyping purposes, it is scalable to mass manufacturing techniques. In this work, we focus on synthesis of unique composite thermoelectric systems optimized for low-temperature applications. We also demonstrate device fabrication techniques for high-density arrays of high-aspect-ratio planar single-element TEGs.

EXPERIMENTAL PROCEDURES

Thermoelectric Materials Synthesis

Elemental Bi (99.999%, 1 mm to 5 mm balls) and Te (99.999%, 1 mm to 12 mm chunks) (Sigma Aldrich Corporation) were selected as starting materials for mechanical alloying. To form mechanically alloyed (MA) *n*-type Bi_2Te_3, a molar ratio of 36:64 of Bi and Te was used.[10] Varying amounts of Se were added from 1 wt.% to 6 wt.% of the total amount of Bi_2Te_3. Previous empirical studies have suggested that an average particle size of 10 μm is needed to achieve optimal composite properties.[11,12] Stainless-steel jars of 100 mL and 10-mm-diameter balls were used for the ball milling process. The ball-to-powder weight ratio was kept at 15:1. All powder handling was performed in an argon-filled glove box, in which the oxygen level was kept below 5 ppm to prevent oxidation of the powders. Mechanical alloying was carried out in a planetary ball mill (QM-4F; Nanjing University, China) at 450 rpm for 16 h in a purified argon atmosphere. The particle size of the as-milled powders was measured using a Coulter LS-100 laser diffraction particle size analyzer. The milled particle size ranged between 2 μm and 200 μm. To further reduce the particle size, the as-milled powders were ball milled again with 3-mm stainless-steel balls at a ball-to-powder mass ratio of 10:1 with isopropyl alcohol (1:1 fluid-to-powder ratio) at 270 rpm for 120 min. The resulting average particle size after ball milling was approximately 10 μm, while the bulk of the particles ranged between 3 μm and 30 μm. XRD was performed on the MA powders to confirm the formation of the desired compound. The XRD pattern of MA *n*-type Bi_2Te_3 with 2% Se is shown in Fig. 2. The peaks suggest the desired formation of MA Bi_2Te_3.[13]

We evaluated conducting polymers poly(3,4-ethylenedioxythiophene) (PEDOT) and polyaniline as potential binders apart from insulating epoxy resin. When using PEDOT as a binder we encountered poor adhesion. The thermoelectric properties of composite film were also inferior when using PEDOT compared with when using epoxy resin as a binder. This was because we needed polymer and active particles in weight ratio of 40:60 when using PEDOT as compared with 20:80 when using epoxy resin in order to make printable inks. We could not use polyaniline as a binder because active particles did not disperse well in the polymer matrix and we could not print it.

An epoxy resin mixture consisting of the resin (EPON 862; Momentive), hardener (MHHPA; Dixie Chemicals), and catalyst (2E4MZCN; Sigma-Aldrich, Inc.) was used as the polymer binder.[14] The thermoelectric inks were prepared using 80 wt.% MA Bi_2Te_3 and 20 wt.% epoxy resin. The slurry was mixed using a vortex mixer and an ultrasonic bath to disperse the particles. The thermoelectric inks

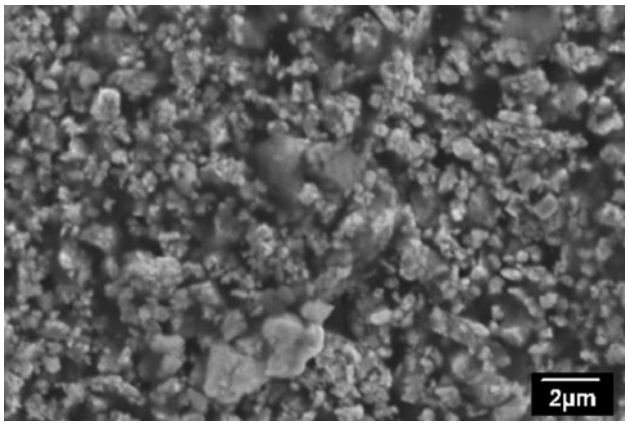

Fig. 3. SEM image of a MA Bi_2Te_3–epoxy composite film.

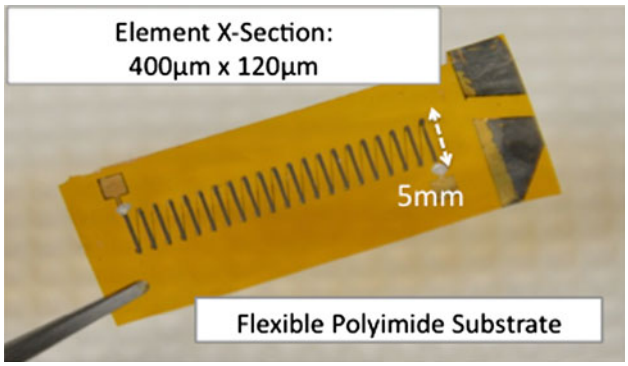

Fig. 4. Image of a printed planar thermoelectric device on a flexible polyimide substrate.

were then printed on glass substrates to form 100-μm- to 200-μm-thick films using the dispenser printer and were cured at 250°C for 12 h to form solid thick films. Figure 3 shows a cross-section SEM image of a Bi_2Te_3–epoxy composite film. The image suggests that the epoxy polymer binder forms a solid, dense matrix when mixed and cured with active Bi_2Te_3 particles. The particle distribution within the film is uniform. No voids are present.

Device Fabrication

Gold metal interconnects (6000 Å thickness) were evaporated onto 50-μm-thick flexible polyimide substrate. Polyimide substrate was chosen due to its flexibility, electrical insulation, high temperature tolerance, and low thermal conductivity (0.12 W/m·K). Next, the MA n-type Bi_2Te_3 composite inks were dispenser printed onto the substrate to form lines spanning across the top to bottom contacts. Finally, the printed lines were cured in an argon/vacuum oven at 250°C. Figure 4 shows an image of the printed thermoelectric lines on a flexible polyimide sheet with evaporated contacts. A 20-element prototype consisting of elements that were 5 mm × 400 μm × 120 μm in dimensions was fabricated and characterized to test performance.

MEASUREMENTS

Electrical resistivity measurements of the printed thermoelectric films were carried out using a standard four-point probe method to determine the sheet resistance of the material. Seebeck measurements were performed using a custom Seebeck testing device to determine the voltage output of the material for a given temperature difference. The thermal conductivity of composite samples was measured by the guarded heat flow meter method at a steady state with a bulk thermal conductivity analyzer (model 2021; Anter Corp.). Relatively larger samples (20 mm × 20 mm × 3 mm) were used for thermal conductivity measurements. The printed prototype device was tested by applying various temperature differences across the device. Temperatures at both ends of the elements were monitored to ensure that a steady state was reached. Once the device reached steady state, the open-circuit voltage of the device was measured using a digital multimeter. A variable load resistance was then connected in series with the device, and voltage measurements were taken at multiple load resistances. The power output was calculated using the measured voltage and load resistance at various temperature differences.

RESULTS

Composite Thermoelectric Thick-Film Characterization

The thermoelectric and thermal transport properties of Se-rich MA Bi_2Te_3 thick films printed on glass substrates using the dispenser printer and cured at 250°C were studied at 20°C to 100°C. Bulk samples of Se-rich MA Bi_2Te_3 were prepared using the cold-pressing method for comparison of the thermoelectric properties.

Figure 5 shows the thermoelectric properties of MA n-type Bi_2Te_3 composite films cured at 250°C as a function of Se percentage. It is clear from the figure that 2% Se results in the highest electrical conductivity and Seebeck coefficient, resulting in the highest power factor. Figure 6 shows the thermoelectric properties of 2% Se MA n-type Bi_2Te_3 composite compared with a bulk sample as a function of temperature. The electrical conductivity is one order of magnitude lower than the bulk value due to the insulating properties of the epoxy polymer present in the composite films. The Seebeck coefficient (α) of the 2% Se MA n-type Bi_2Te_3 composite has a peak value of approximately 200 μV/K when cured at 250°C, which is similar to that of the bulk 2% Se MA Bi_2Te_3 sample. However, the MA Bi_2Te_3 composites exhibit fairly low thermal conductivity (0.27 W/m·K) due to the insulating effects of the polymer. The ZT value of the Bi_2Te_3 composite ultimately reaches 0.17 with efficiency losses due to the lower electrical conductivity of the system.

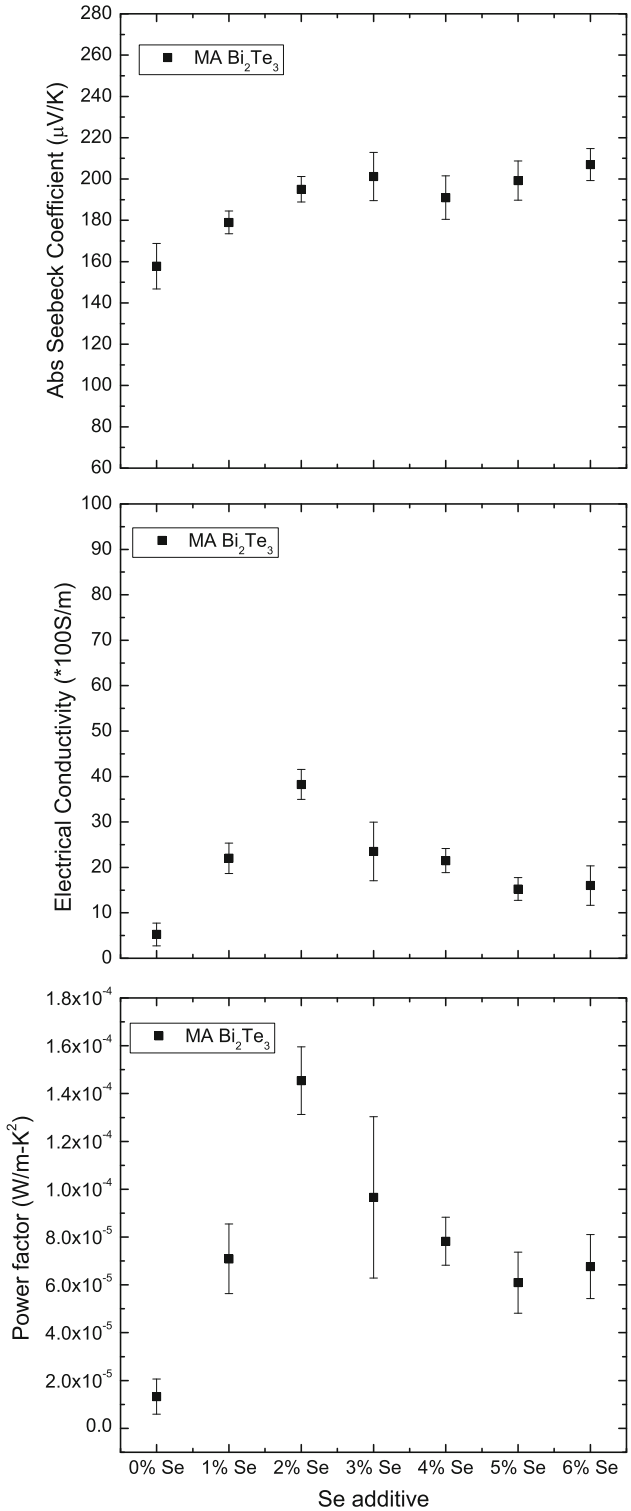

Fig. 5. Thermoelectric properties of MA *n*-type Bi_2Te_3 composite films cured at 250°C as a function of % Se additive.

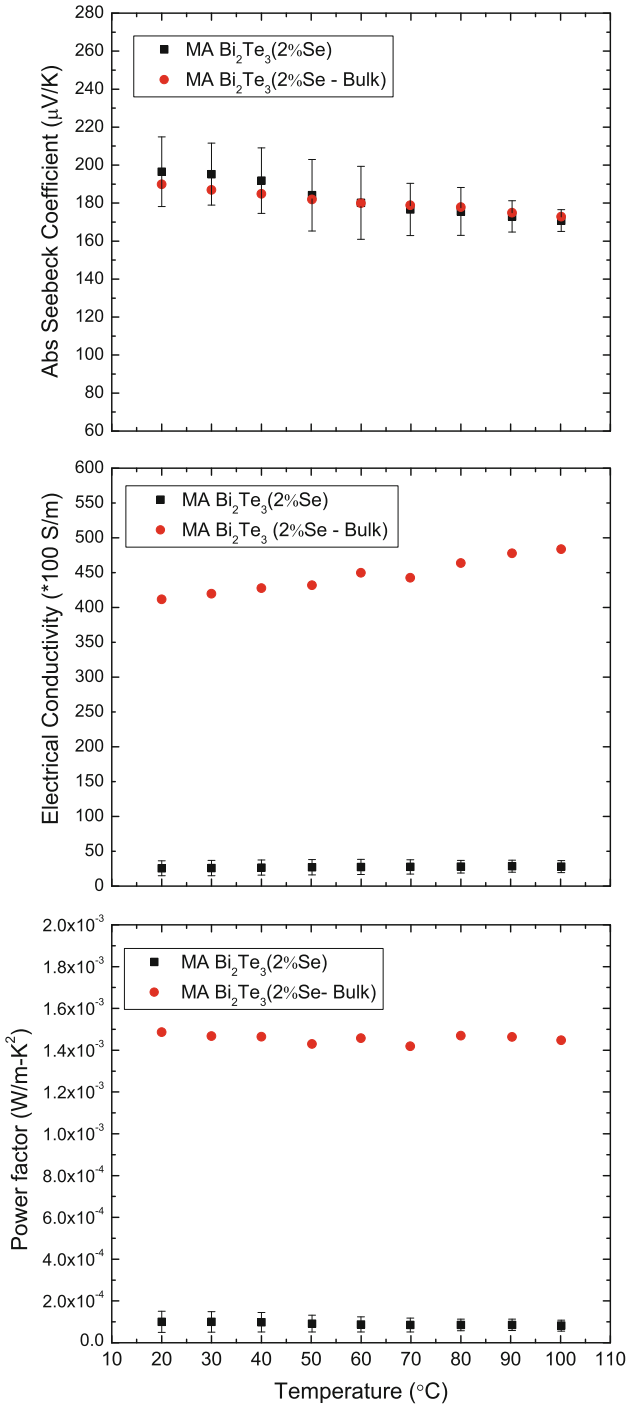

Fig. 6. Thermoelectric properties of 2% Se MA *n*-type Bi_2Te_3 composite and bulk sample as a function of temperature.

Prototype Device Characterization

The measured device resistance of the 20-element prototype was 1.0 kΩ. The maximum power output of the device occurs when the load resistance matches the device resistance. The device resistance, however, is much higher than the expected resistance calculated from the material properties. This discrepancy is likely due to high contact resistance at the electrical interconnects. Figure 7 shows the measured power density of the device as a function of temperature difference. Maximum power output at matched load resistance was measured at ΔT of 5 K, 10 K, and 20 K. The solid line in the figure

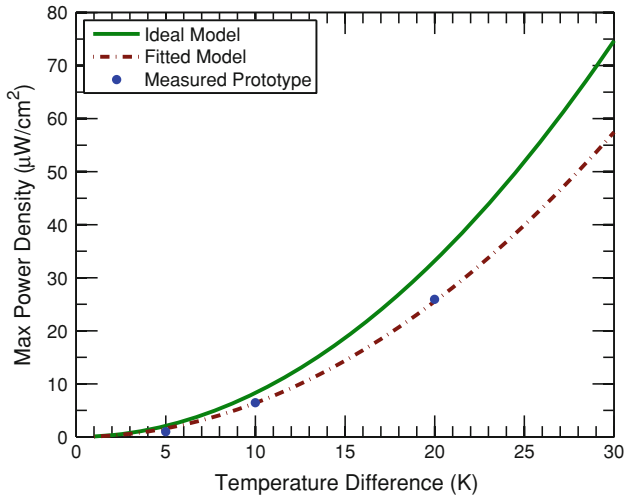

Fig. 7. Power density of the device as a function of temperature difference.

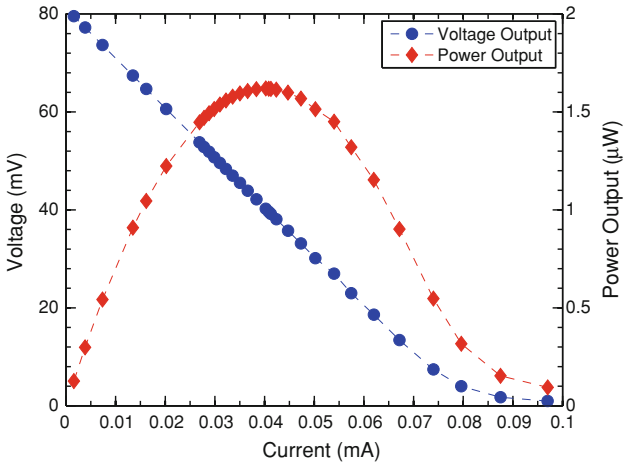

Fig. 8. Characteristic curves for the prototype device at ΔT = 20 K.

indicates the ideal model, while the dashed line indicates the fitted model.[15,16]

Figure 8 shows the device characteristic curves for the prototype device at ΔT = 20 K. The open-circuit voltage of the device at ΔT = 20 K was measured to be 80 mV. The load resistance was varied, and corresponding voltages were measured. Current and power were calculated for each applied load resistance and respective measured voltage. The device characteristic curve plots calculated current on the x-axis, measured voltage on the primary y-axis, and calculated power on the secondary y-axis. At matched load resistance, the device produces a maximum output power of approximately 1.6 μW at 40 μA and 40 mV.

DISCUSSION

The MA n-type Bi_2Te_3 material synthesized in this work proves to be promising for printed thermoelectric devices. While the efficiencies of the composite materials do not exceed that of state-of-the-art thermoelectric materials,[1,17] its advantages in processing and rapid fabrication provide implementation and deployment advantages over many complex materials. Future work on composite materials development can further take advantage of printed methods for manufacturing TEGs while improving the efficiency. Recent advances have already spurred growing interest in thermoelectric materials utilizing conductive polymers and their composites.[18–20]

The prototype shown in this work demonstrated a cross-sectional power density of 25 μW/cm^2 for a 20 K temperature difference. Based on current material properties, an ideal device is capable of providing a power density of 35 μW/cm^2 for ΔT = 20 K. Optimization of device design, fabrication, and materials processing will be further investigated to improve device performance. The element dimensions of the prototype were chosen for demonstration purposes and ease of printing. Future work will aim to improve the device design and efficiency while lowering device resistance overall.

CONCLUSIONS

In this work we successfully synthesized printable MA n-type Bi_2Te_3 materials for fabrication of planar high-density array and high-aspect-ratio TEGs. Optimization of materials processing yielded a ZT value of 0.17 for the n-type composite. A 20-element planar prototype device was printed on a flexible polyimide substrate. The device produced 1.6 μW at 40 mV and 40 μA for a 20 K temperature difference, with losses from device resistance. These results indicate a device power density of 25 μW/cm^2. The results demonstrate the feasibility of utilizing MA n-type Bi_2Te_3 with 2% Se composites for single-element thermoelectric devices. These results are promising for low-cost and scalable TEGs for various low-power energy harvesting applications. Further work will continue to optimize MA n-type materials and perhaps explore a complementary p-type material to fabricate a TEG.

ACKNOWLEDGEMENTS

The authors thank the California Energy Commission for supporting this research under award DR-03-01. We would also like to thank Rei Chang Juang, Jay Keist, Brian Mahlstedt, Michael Nill, and Jonathan Brown for their contributions.

REFERENCES

1. G.J. Snyder and E.S. Toberer, *Nat. Mater.* 7, 105 (2008).
2. D.M. Rowe, *Thermoelectrics Handbook: Micro to Nano* (Boca Raton: Taylor and Francis, 2005).
3. W. Glatz, E. Schwyter, L. Durrer, and C. Hierold, *J. Micromech. Microeng.* 18, 763 (2009).
4. J. Weber, K. Potje-Komloth, F. Haase, P. Detemple, F. Volklein, and T. Doll, *Sensors Actuators A* 132, 325 (2006).

5. K. Gilleo, *Polymer Thick Film* (New York: Thomson, 2006).
6. K. Miyazaki, T. Lida, and H. Tsukamoto, *Proceedings of 22nd International Conference on Thermoelectrics* (France, 17–21 August, 2003), p. 641.
7. C.C. Ho, J.W. Evans, and P.K. Wright, *Proceedings of Ninth Power MEMS Workshop* (2009), p. 141.
8. C.C. Ho, D. Steingart, J.W. Evans, and P.K. Wright, *ECS Trans.* 16, 35 (2008).
9. E.S. Leland, P.K. Wright, and R.M. White, *J. Micromech. Microeng.* 19, 094018 (2009).
10. H.J. Goldsmid and R.W. Douglas, *Br. J. Appl. Phys.* 5, 386 (1954).
11. A. Chen, M. Koplow, D. Madan, P.K. Wright, and J.W. Evans, *Proc. ASME Conf.* 12, 343 (2009).
12. A. Chen, D. Madan, P.K. Wright, and J.W. Evans, *J. Micromech. Microeng.* 21, 104006 (2011).
13. L.D. Zhao, B.P. Zhang, J.F. Li, M. Zhou, and W.S. Liu, *Phys. B* 400, 11–15 (2007).
14. D. Madan, A. Chen, P.K. Wright, and J.W. Evans, *J. Appl. Phys.* 109, 034904 (2011).
15. W. Glatz, S. Muntwyler, and C. Hierold, *Sensors Actuators A Phys.* 132, 337 (2006).
16. M. Strasser, R. Aigner, C. Lauterbach, T.F. Sturm, M. Franosch, and G. Wachutka, *Sensors Actuators A* 114, 362 (2004).
17. C.J. Vineis, A. Shakouri, A. Majumdar, and M.G. Kanatzidis, *Adv. Mater.* 22, 3970 (2010).
18. O. Bubnova, Z.U. Khan, A. Malti, S. Braun, M. Fahlman, M. Berggren, and X. Crispin, *Nat. Mater.* 10, 429 (2011).
19. K.C. See, J.P. Feser, C.E. Chen, A. Majumdar, J.J. Urban, and R.A. Segalman, *Nano Lett.* 10, 4664 (2010).
20. B. Zhang, J. Sun, H.E. Katz, F. Fang, and R.L. Opila, *ACS Appl. Mater. Interfaces* 2, 3170 (2010).